International Journal of Nanomedicine

Dovepress
open access to scientific and medical research

Open Access Full Text Article

ORIGINAL RESEARCH

Arthrospira platensis Nanoparticles Mitigate Aging-Related Oxidative Injured Brain Induced by D-galactose in Rats Through Antioxidants, Anti-Inflammatory, and MAPK Pathways

Heba I Ghamry[1,*], Mustafa Shukry[2,*], Mohamed A Kassab[3], Foad A Farrag[4], Nagi M El-Shafai[5], Enas Elgendy[6], Amany N Ibrahim[7], Salwa A Elgendy[7], Ali Behairy[7], Samah F Ibrahim[8], Florin Imbrea[9], Crista Florin[10], Mohamed Abdo[11,12], Inas A Ahmed[13], Marwa H Muhammad[14], Hala Anwer[14], Ahmed Abdeen[15]

[1]Nutrition and Food Science, Department of Home Economics, Faculty of Home Economics, King Khalid University, Abha, 61421, Saudi Arabia; [2]Department of Physiology, Faculty of Veterinary Medicine, Kafrelsheikh University, Kafrelsheikh, Egypt; [3]Department of Histology, Faculty of Veterinary Medicine, Kafrelsheikh University, Kafrelsheikh, Egypt; [4]Department of Anatomy and Embryology, Faculty of Veterinary Medicine, Kafrelsheikh University, Kafrelsheikh, Egypt; [5]Nanotechnology Center, Chemistry Department, Faculty of Science, Kafrelsheikh University, Kafrelsheikh, Egypt; [6]Histology and Cell Biology Department, Faculty of Medicine, Benha University, Benha, Egypt; [7]Department of Pharmacology, Faculty of Medicine, Benha University, Benha, Egypt; [8]Department of Clinical Sciences, College of Medicine, Princess Nourah bint Abdulrahman University, Riyadh, 11671, Saudi Arabia; [9]Department of Biology and Plant Protection, Faculty of Agriculture, University of Life Sciences "King Michael I" from Timişoara, Timisoara, 300645, Romania; [10]Department of Soil Science, Faculty of Agriculture, University of Life Sciences "King Michael I" from Timişoara, Timisoara, 300645, Romania; [11]Department of Animal Histology and anatomy, School of Veterinary Medicine, Badr University in Cairo (BUC), Badr City, Egypt; [12]Department of Anatomy and Embryology, Faculty of Veterinary Medicine, University of Sadat City, Sadat City, Egypt; [13]Department of Medical Biochemistry and Molecular Biology, Faculty of Medicine, Benha University, Benha, Egypt; [14]Department of Physiology, Faculty of Medicine, Benha University, Benha, Egypt; [15]Department of Forensic Medicine and Toxicology, Faculty of Veterinary Medicine, Benha University, Toukh, Egypt

*These authors contributed equally to this work

Correspondence: Mustafa Shukry, Department of Physiology, Faculty of Veterinary Medicine, Kafrelsheikh University, Kafrelsheikh, Egypt, Tel +20-10-20705320, Email mostafa.ataa@vet.kfs.edu.eg; Crista Florin, Department of Soil Science, Faculty of Agriculture, University of Life Sciences "King Michael I" from Timişoara, Timisoara, Romania, Email florin_crista@usab-tm.ro

Background: Loss of normal function is an inevitable effect of aging. Several factors contribute to the aging process, including cellular senescence and oxidative stress.

Methods: We investigate how *Arthrospira platensis* Nanoparticles (NSP) protect against aging injury induced by d-galactose (D-gal) in the rat. So, we subcutaneously (S/C) injected D-gal at 200 mg/kg BW to see if Arthrospira platensis Nanoparticles (NSP) might protect against the oxidative changes generated by D-gal. NSP (0.5 mg/kg body weight once daily by gastric gavage) was given to all groups apart from the control and D-gal groups. The d-gal + NSP group was supplemented with 200 mg of D-gal per kg BW once a day and NSP 0.5 mg/kg BW given orally for 45 days. Biochemical, mRNA expression, and histological investigations of brain tissues were used to evaluate the oxidative alterations caused by d-gal and the protective role of NSP.

Results: Our data demonstrated that d-gal was causing significant reductions in relative brain and body weight with increased malondialdehyde (MDA) and redox oxygen species (ROS) levels and increases in serum creatine phosphokinase (CPK) and creatine phosphokinase isoenzyme BB (CPK-BB) with marked decreases in the level of antioxidant enzyme activity in the brain and acetylcholinesterase activity augmented with a phosphorylated H2A histone family member X (γ-H2AX) level increased. The D-gal group had considerably higher phosphorylated p38 mitogen-activated protein kinases (P38MAPK) and C-Jun N-terminal (JNK) kinases. The d-gal administration stimulates the apoptotic gene expression by downregulating the brain superoxide dismutase (SOD), catalase (CAT), and nuclear factor erythroid 2–related factor 2 (Nrf2). The NSP administration saved these parameters in the direction of the control. The brain histopathologic and immunohistochemistry analysis findings support our findings on NSP's protective role.

Conclusion: The NSP may be a promising natural protective compound that can prevent aging and preserve health.

Keywords: aging, antioxidants, MAPK, Nrf2, oxidative stress

Received: 28 April 2023
Accepted: 14 September 2023
Published: 2 October 2023

Introduction

The increase of reactive oxygen species (ROS) and decreased antioxidant capabilities are two significant contributors to the deterioration that characterizes the aging process.[1] When looking for anti-aging medications, the d-galactose (D-gal)-induced aging model is frequently employed.[2] Proteins and peptides include free amines that can react with D-gal when it build up in the body, producing advanced glycation end products (AGEs).[3] Therefore, AGEs engage with particular receptors (RAGE) in numerous cell types, inducing the activation of the downstream nuclear factor kappa B (NF-κB), leading to ROS formation, which may hasten the aging process.[4] Increased levels of ROS, such as superoxide anion and nitric oxide, cause cellular damage in proteins, lipids, and DNA that can promote the development of various diseases.[5,6] Antioxidants derived from natural sources are gaining popularity to protect cells from oxidative damage and reduce the production of harmful free radical species.[7] Spirulina is the common name for the fresh blue-green algae *Arthrospira platensis*, a filamentous cyanobacterium rich in phytochemical components such as essential amino acids and lipids. Carotenoids, other pigments, and riboflavin, a B vitamin, are all present.[8] Aspergillus is a significant contributor of fungal secondary metabolites, which have several biological applications.[9] Anticancer and antioxidant activities are hallmarks of *A. awamori* supplementation, which also boosts growth efficiency and reduces lipid peroxidation in skeletal muscle.[10,11] *A. awamori* contained high levels of several compounds with antioxidant action, including coumarins, glucose, saponins, flavonoids, and tannins.[12] Because of their small size and active surface, nanoparticles are unlike any other active chemical; unlike traditional particles, they can remain in the bloodstream for a longer time, resulting in high and effective activity.[13] This paper investigates the potential intracellular pathway by which A. platensis nanoparticles ameliorate D-gal-induced aging harm in male rats. To assess if NSP has antioxidant capability, we looked at its effects on the oxidative alterations brought on by the D-gal-aging model in the brains of rats.

Ethical Guidelines

The Animal House Ethical Committee at Kafrelsheikh University's School of Veterinary Medicine in Egypt approved all of the experiments in this study (Code. VKSU 01/3/22). The rats were cared for following the ethical guidelines established by the National Institutes of Health (NIH).

Animal

Thirty-six male Wistar rats weighing 155± 2 g were utilized in this experiment. Tweleve h of darkness and 12 hof light, with ad libitum food and water. All experiments were conducted following the standards set forth by the ethical committee of Egypt's Kafrelsheikh University. The rats were treated humanely following National Institutes of Health recommendations. Rats were adapted for ten days before the experiments. The ingredients of the basal diet follow Atta et al[14]

Preparation of Nanoparticles of Arthrospira Platensis (NSP)

Algae Biotechnology Unit in Giza, Egypt, gave us 1 g of *A. spirulina*. After being suspended for an hour in 100 mL of distilled water with stirring, the suspension was warmed at 50 for three hours, and the ultrasonication process was performed to high dispersion and more extract purity. The addition of 5g of the spirulina extract to 50 mL of 0.5 g synthesized Se NPs, which was prepared by the precipitation method by reduction process of the sodium selenite solution through hydrazine hydrochloride as a reducing reagent, and the Se NPs formed after washing and drying. The addition of Se NPs to the spirulina extract for shrinking the spirulina particles and giving it in the nanoscale. The mixture was ultrasonicated for 1 h, then left stirring overnight at room temperature, the obtained spirulina nanoparticle was centrifugated. The resultant was washed and dried, then characterized with different techniques such as scanning electron microscopy (SEM), X-ray diffraction (XRD), dynamic light scattering (DLS), and UV-Vis spectroscopy (UV-Vis). The synthesized NSP diameter appeared at 158 nm. (See Figure 1S. Scanning electron microscopy-energy dispersive X-ray analysis (SEM-EDX) of NSP).

Experimental Protocol

Rats were randomized into four groups (9 rats /group), with the control group receiving distilled water via a stomach tube and a subcutaneous (S/C) injection of physiological saline solution (0.9%); the D-gal group receiving a S/C injection of 200 mg per kg /BW of D-gal dissolved in saline solution daily for 45 days;[15,16] in addition to the third group, the rats were received NSP (0.5 mg/kg body weight),[17] one time daily using the stomach tube. The fourth group co-treated with both D-gal+ NSP using the dose mentioned above for 45 days using the stomach tube.

Blood and Tissue Sample

After the experiment, the rats were given an intravenous dose of pentobarbital (30 mg/kg).[14] Serum was extracted from blood samples by centrifuging at 5000 RPM for 15 min. Histopathology and immunohistochemistry analyses were performed on rat brains after they were washed in phosphate buffer saline (PBS, pH 7.4) and preserved in 4% paraformaldehyde dissolved in PBS for 48 h. Other brain regions frozen at −80 °C can be used for gene expression analysis.

Biochemical Analysis and Brain Oxidative Stress Markers

The serum CPK and CPK-BB activities were measured using commercially available diagnostic kits from Biodiagnostic Co., Egypt. The measurement was performed spectrophotometrically, following the instructions provided by the manufacturer. The γH2AX levels in brain tissue homogenate were measured using an ELISA method. The ELISA kit used for this analysis was supplied by Sun Red Biotechnology Co. (Shanghai, China) with the catalog number #: 201-11-1762.

Brain homogenates were analyzed for oxidative damage after being preconditioned in PBS. GSH levels activity were evaluated following Beutler et al[18] using (Biodiagnostic, Giza, Egypt) which utilizes the reduction of 5,5 dithiobis 2-nitro-benzoic acid (DTNB) by glutathione. The resulting product was then measured at a wavelength of 405 nm. The measurement of superoxide dismutase (SOD) activity involves the utilization of xanthine and xanthine oxidase to produce superoxide radicals. These radicals then react with 2-(4-iodophenyl)-3-(4-nitrophenyl)-5-phenyltetrazolium chloride, forming a red formazan dye. This reaction's inhibition level determines the activity of superoxide dismutase following Flohe[19] using a ready-to-use kits (Biodiagnostic, Giza, Egypt). CAT activity was measured using a colorimetric method based on Aebi's [20] approach. Each CAT unit decomposed one μM of H_2O_2 per min at 25 °C and pH 7.0. The reaction involved CAT reacting with known amount of H_2O_2, which was then stopped after 1 min using a CAT inhibitor. The remaining H_2O_2 reacted with specific reagents to form a color that indicated the CAT level. Enzyme activities were expressed as unit/mg protein following Aebi's protocol[20] using a commercial kits (Biodiagnostic, Giza, Egypt). The total antioxidant capacity was assessed by measuring the depletion of hydrogen peroxide due to the presence of antioxidants in the sample. The remaining H_2O_2 was quantified using a calorimetric enzymatic reaction, which involved converting 3.5-dichloro-2-hydroxy benzenesulfonate to a product.[21] Thiobarbituric acid was used to measure malondialdehyde, an intermediate lipid peroxidation product.[22] Calorimetric analysis of Sigma-Aldrich acetylcholinesterase (AChE) in the brain (St Louis, MO, USA) was performed according to the method developed by Den Blaauwen et al[23] This method involves the hydrolysis of acetylcholine by acetylcholinesterase, resulting in the production of acetate and thiocholine. In the presence of dithiobis-nitrobenzoate, thiocholine reacts to produce 2-nitro mercapto benzoate, which can be quantitatively measured at a wavelength of 405 nm.

The brain tissue homogenate was tested for reactive oxygen species (ROS) by Socci et al[24] Using a fluorescence plate reader and an excitation wavelength of 488 nm, 2.7-dichlorofluorescein diacetate can be converted to the fluorescent compound 2.7-dichlorofluorescein, which emits light at a wavelength of 525 nm. Protein concentration in homogenates was measured using the Bradford assay (Bio-Rad Laboratories, Watford, UK).[25] The c-Jun N-terminal kinase (JNK) ELISA Kit and p38 mitogen-activated protein kinase (P38MAPK) ELISA kit, provided by MyBioSource in San Diego, California, USA, were used for the measurement of JNK and P38MAPK levels, respectively.

Gene Expression

Gene expression in the brain was studied by reverse transcription-polymerase chain reaction. About 100 mg of brain tissue was weighed, and TRIzol was used to extract total RNA (Invitrogen, Life Technologies, Carlsbad, CA, USA). The RNA samples had an A260/A280 ratio greater than 1.8 and used a cDNA kit (Fermentas, Waltham, MA, USA). The

SYBR Green master mix and primers listed in Table 1S were used to amplify with the glyceraldehyde-3-phosphate dehydrogenase (GAPDH) control (housekeeping) gene. We used two methods to analyze the amplification data.[26]

Brain Histological Analysis

For 24 h, brain samples were submerged in a neutral formaldehyde buffer solution (1%). (Sigma-Aldrich). Tissues have been fixed using a paraffin integration device after undergoing ethanol dehydration (Sigma-Aldrich).[27] Following Malkiewicz et al[28] Paraffin wax was used to embed the dried (10%) brain tissue samples. It was sliced into six even thicknesses, placed on glass slides, and incubated for a whole day. After 30 min in a protein block, slices were transferred to a 4 °C refrigerator overnight to be incubated with a polyclonal anti-GFAP antibody (1:1000). After 30 min at room temperature in a solution of avidin-biotin-peroxidase reagent and biotinylated anti-rabbit IgG antibody (1:100), sections were stained. The peroxidase response was observed using DAB. Hematoxylin was used to contrast the Nissl-stained samples that were used to see the neurons.

Statistical Assessment

GraphPad Prism was used to conduct a one-way analysis of variance followed by Tukey's post hoc tests on the collected data (Version 8.4.3). A statistical significance level of $P < 0.05$ was determined. The inter-variable correlation heatmap, inter-intervention clustering heatmap, and VIP ratings were all generated in RStudio (R version 4.0.2).

Results

Patterns of Spirulina and NSP

Figure 1 illustrated the formation of nano spirulina (NSP), XRD patterns (Figure 1a) were detected at 20, 37, 44, 65, and 79° for spirulina. At the same time, the NSP has a crystal structure at 23, 27, 41, 43, 45, 51.55, and 60°. The shift and crystallinity of the NSP emphasized the formation of NSP. Zeta potential experiment was performed in double distilled water and room temperature conditions; the diluted solution of the examined samples was used to investigate the investigated samples' stability and distribution (Figure 1b). The electrostatic stability around values ± 30 refers to the dispersion and stability of the NSP that has −21 mV. Dynamic light scattering (DSL) was performed to determine the particle size of NSP, which appeared in diameter at 158 nm (Figure 1c); the sample was prepared in double distilled water and at room temperature. In addition, the SEM micrograph displayed the surface of the synthesized NSP, which NSP nanoparticles accumulated on the surface (Figure 1d).

Stability and Distribution of NSP in situ and Tissue

Figure 2a illustrates the synthesized NSP's absorption peaks displayed by UV-Vis spectroscopy for prepared solution in double distilled water and room temperature conditions. The measuring was performed at different time after 120 hwhich is the period of measuring the nano spirogyra has high stability and high dispersion; this result qualifies and supports it for good distribution during biological activity within the blood and tissues. Zeta potential was performed to investigate the stability and distribution of NSP, the electrostatic stability around values from ± 30 referred to the dispersion stability of the NSP. The cyclic voltammetry (CV) was performed to display the stability and distribution of NSP, where 5 mg stock of examined samples was dispersed in 10 mL in double distilled water and measured by CV analysis under measurement conditions at room temperature, 0.1 Vs-1 scan rate, 0.1M of electrolyte solution from potassium chloride salt (KCl). The CV technique was performed with different scan rates to emphasize the stability of the NSP and good dispersion in situ and tissue (Figure 2b). In addition, the Tafel plot was calculated to illustrate the stability of NSP with different scan rates and 100-cycle measurements (Figure 2c). The surface area under the curve of the CV curve, which can be computed using Eq. 1 below,

$$C_{area} = \frac{\int_{V_a}^{V_b} idV}{S\upsilon(V_b - V_a)} \quad (1)$$

The higher surface area and the conductivity of the fabricated electrode cause the higher area under the CV curve, in addition to enhancing the porosity of the surface. The C_{area} was displayed at 190 $mFcm^{-2}$ because of the surface area and

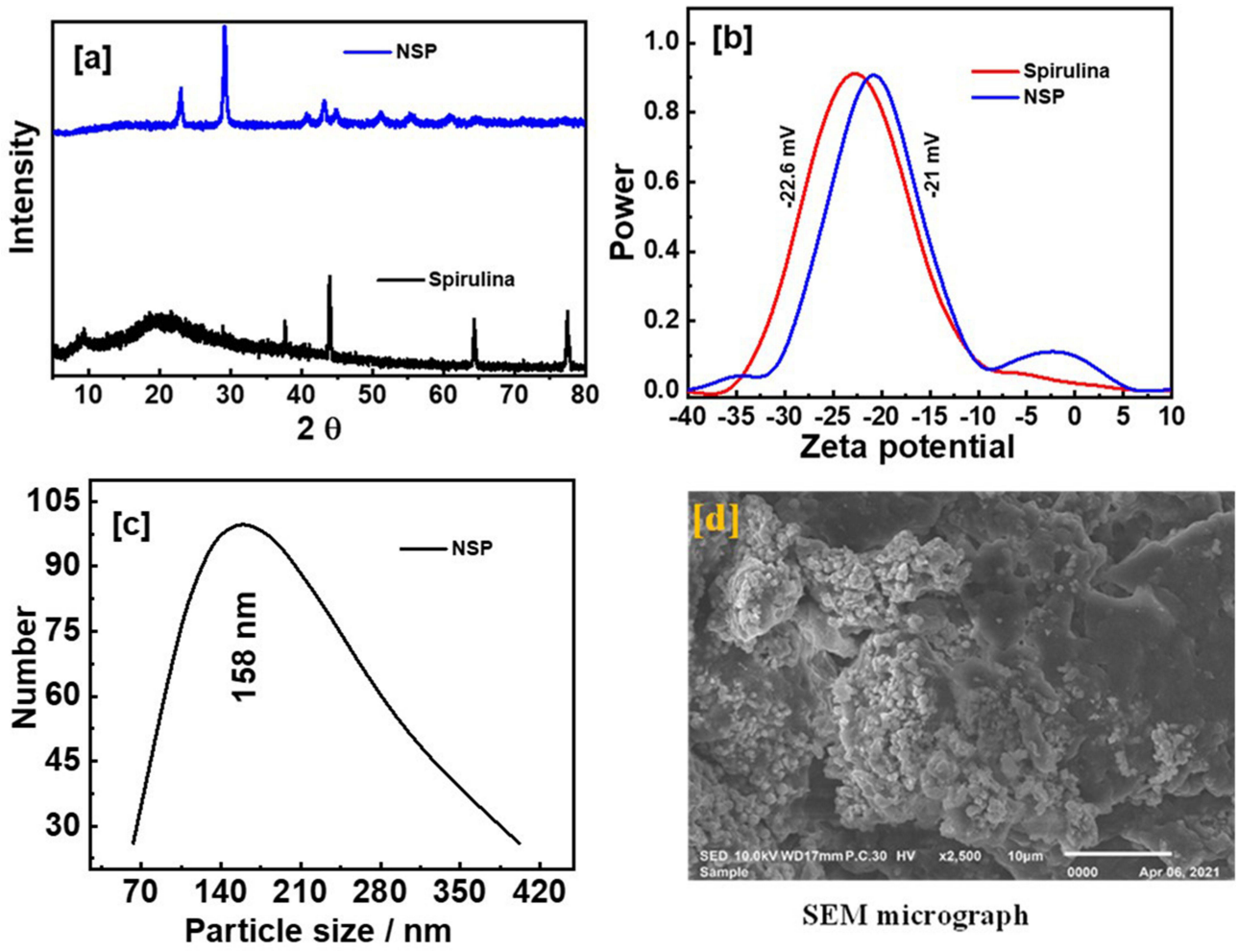

Figure 1 XRD patterns of spirulina and NSP (**a**), zeta potentials of spirulina and NSP (**b**), DLS of NSP (**c**), and SEM micrograph of NSP (**d**).

high conductivity of the NSP. More than 100 cycles of nano spirogyra with scan rate 0.1 Vs-1 were measured to estimate the stability, distribution, and long cycling electrochemical properties (Figure 2d). The cycle stability (85%).

Body Weight

It can be seen in Table 1 that when NSP-treated rats were given the D-gal, their brain weight increased both absolutely and in comparison to that of D-gal indvidual treatment. The D-gal group lost significantly more weight than the other treatment groups ($P < 0.05$). However, compared to D-gal-treated rats, NSP-adminstrated animals showed a dramatic rise in body weight. There were no deaths in any of the experimental groups.

Oxidative Injury and Antioxidant Markers

As shown in Figure 3 D-gal-induced ageing significantly ($P < 0.01$) increased MDA compared to the other treatment animals. Brain homogenate MDA and ROS MDA levels were significantly lower in the D-gal+NSP group compared to the D-gal group ($P < 0.05$). SOD, Catalase, GSH, and TAC levels were considerably higher in the D-gal+NSP group than in the D-gal-treated group.

Biochemical Parameters and Acetylcholinesterase Activity

Compared to the other treated groups, Figure 4 shows that serum CPK and CPK-BB levels, as well as brain acetylcholinesterase activity and γ-H2AX 1 levels, were significantly elevated ($P < 0.05$) in d-gal-treated rats. These

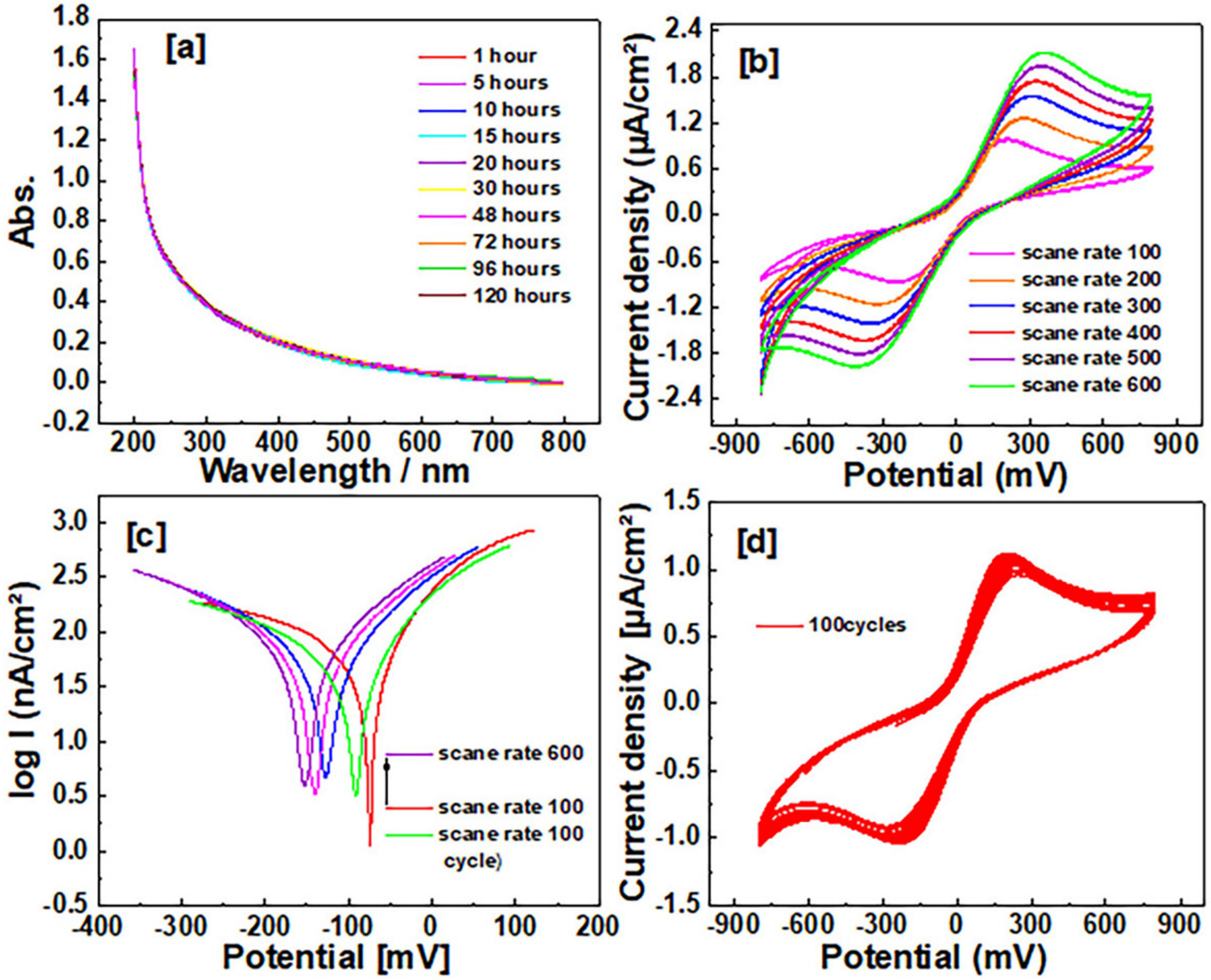

Figure 2 Stability and distribution of NSP in situ and tissue: (**a**) Illustrates the synthesized NSP's absorption peaks displayed by UV-Vis spectroscopy. (**b**) The stability of the NSP and good dispersion in situ and tissue. (**c**) The stability of NSP with different scan rates with 100 cycle measurements. (**d**) The stability, distribution, and long cycling electrochemical properties.

settings were saved in the NSP administration's master control database. P38 MAPK and C-Jun N-terminal kinase (JNK) phosphorylation levels were significantly more significant in the D-gal group compared to the other treatment groups. The NSP therapy considerably suppressed this increase in the D-gal group, as seen in Figure 5A and B, respectively.

Table 1 Influence of NSP on the Aging Rat Brain and Body

	Control	D-gal	NSP	D-gal+NSP
Body weight (g, Initial)	156.17±4.2	157.7±4.5	152±4.2	157.75±3.5
Body weight (g, Final)	232.01±4.5^{a}	201.81±5.1^{c}	234.1±2.1^{a}	221.2±5.1^{b}
Weight gain (g)	75.84±2.1^{a}	44.12±2.2^{c}	82.1±3.2^{a}	63.45±2.2^{b}
Brain weight (g, Absolute)	1.98±0.01^{a}	1.17±0.02^{bc}	2.014±0.02^{a}	1.65±0.02^{b}
Brain weight (%, Relative)	0.855±0.01^{a}	0.5797±0.01^{c}	0.860±0.01^{a}	0.745±0.02^{b}

Notes: Data showed as mean ± S.E.M. $^{a, b, c}$Data from the same raw that had different letters considerably varied. $P < 0.05$. (g), gram. (%), percent. (n =9).

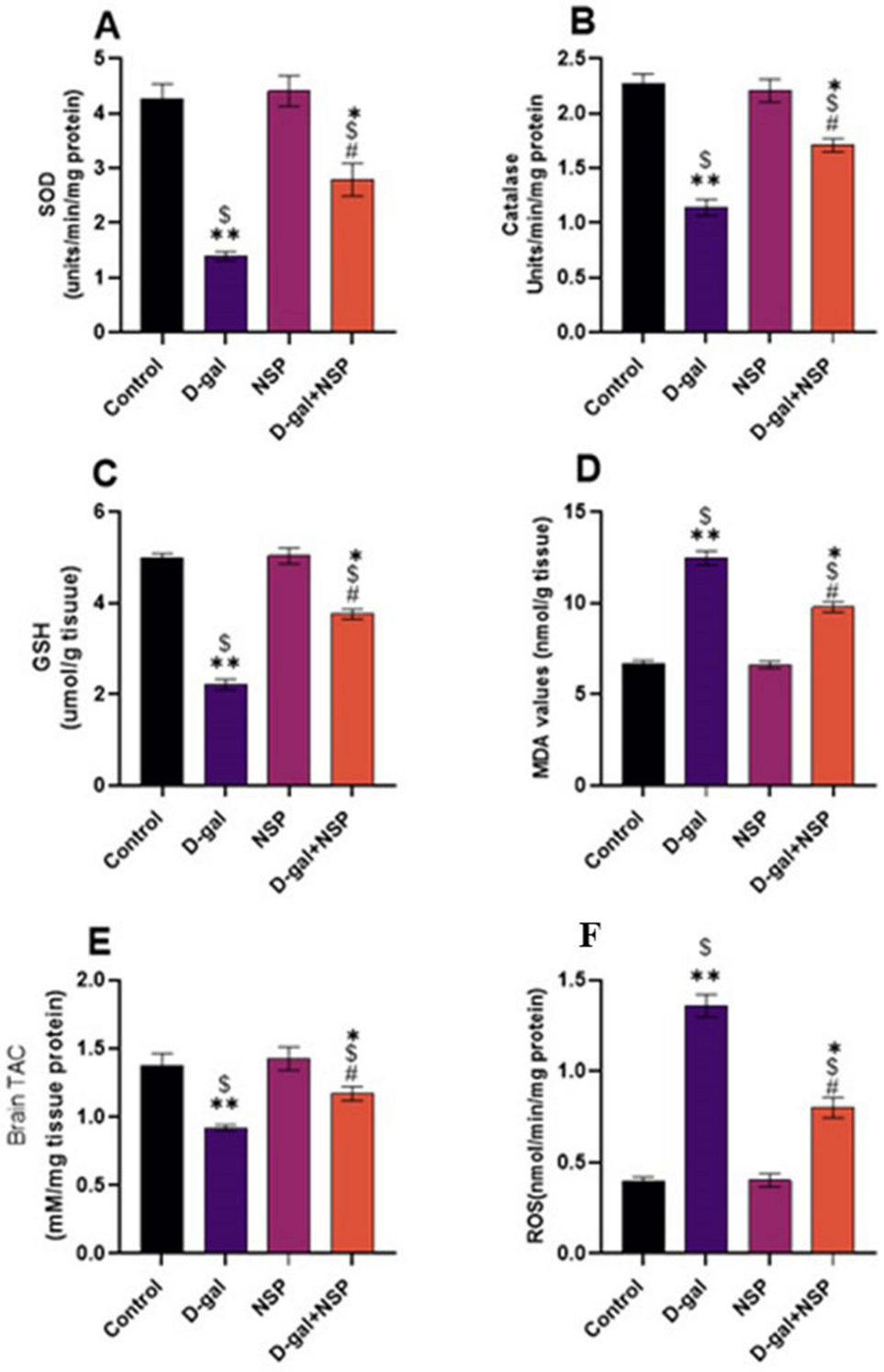

Figure 3 Brain antioxidant markers. (**A**) SOD. (**B**) Catalase. (**C**) GSH. (**D**) MDA. (**E**)TAC. (**F**) ROS. Data showed as Mean ± SEM. *P < 0.05, **P < 0.01 vs the control. $P < 0.01 vs the NSP, #P <0.05 vs the D-gal. n= 9.

Genes Expression

Brain mRNA expression of superoxide dismutase (SOD), catalase (CAT), and nuclear factor (Nrf2) was considerably lower in the D-gal treated group compared to the other treated group (Figure 6). In D-gal+NSP-treated animals, this expression level was normalized considerably (P < 0.05). Bax mRNA expression was significantly higher in the d-gal

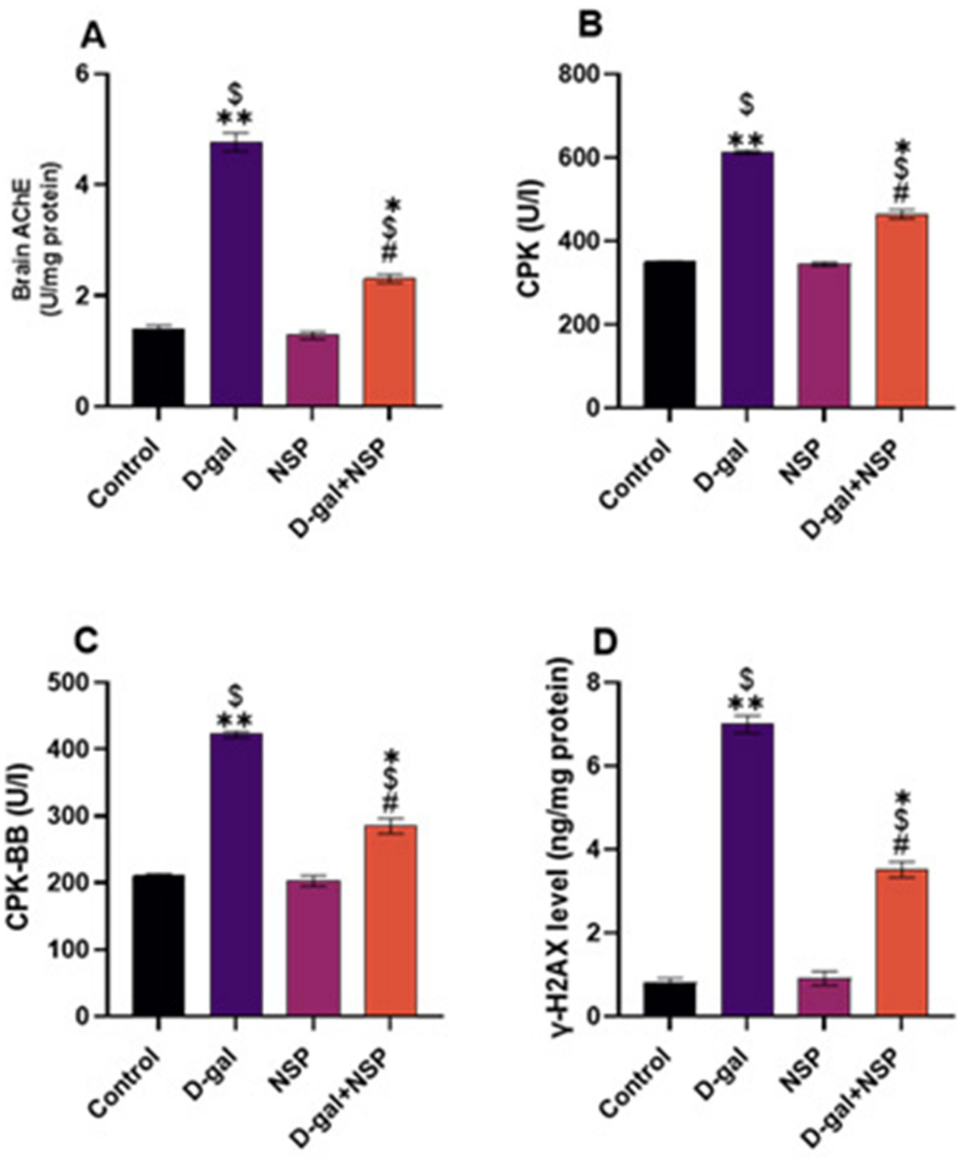

Figure 4 Effect of the NSP on AchE activity (**A**), serum CPK (**B**), CPK-BB (**C**), and γ-H2AX level (**D**). Data showed as Mean ± SEM. *P < 0.05, **P < 0.01 vs the control. $P < 0.01 vs the NSP, #P <0.05 vs the D-gal. (n= 9).

group than in the other treatment group (P< 0.01). However, Bax mRNA expression was significantly decreased in the D-gal+NSP-treated group. Besides, compared to the D-gal-treated group, Bcl2 expression was considerably higher in the D-gal+NSP group. Compared to the other treated group, the NSP treatment normalized the p21 mRNA expression in the brain of the D-gal group (P < 0.01).

Correlation Heatmap and Scores of the Variable Important Project (VIP)

The correlation heatmap illustrated in Figure 7A offered an intuitive visualization of results obtained from all treatment groups, which summarizes the correlation between all measured biochemical variables and mRNA expression of target genes in response to D-gal and/or NSP treatments. A colored scale from highest to lowest, with red denoting a positive association and blue indicating a negative correlation. The intensity of the hue conveys the degree of correlation. According to Pearson's correlation coefficient between all measured factors, the various squares are colored. These data exhibit strong positive correlations between the variable decreased along each other's, including the tissue SOD, CAT, GSH, and TAC levels, and the mRNA expression of SOD, CAT, Nrf2, and Bcl2. In addition to

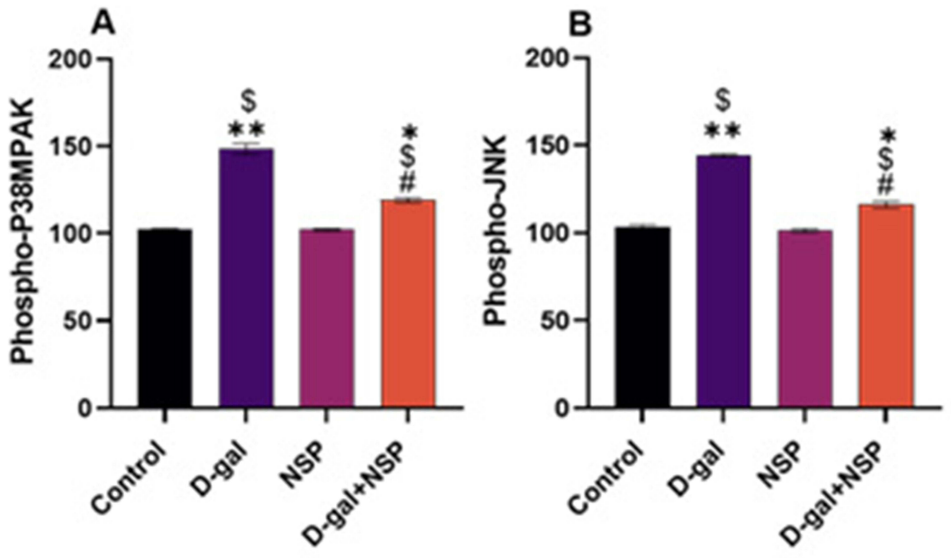

Figure 5 Effect of the NSP on (**A**). Phospho-P38MAPK. (**B**) Phospho-JNK proteins. Data showed as Mean ± SE. *P < 0.05, **P < 0.01 vs the control. $P < 0.01 vs the NSP, #P <0.05 vs the D-gal. (n= 9).

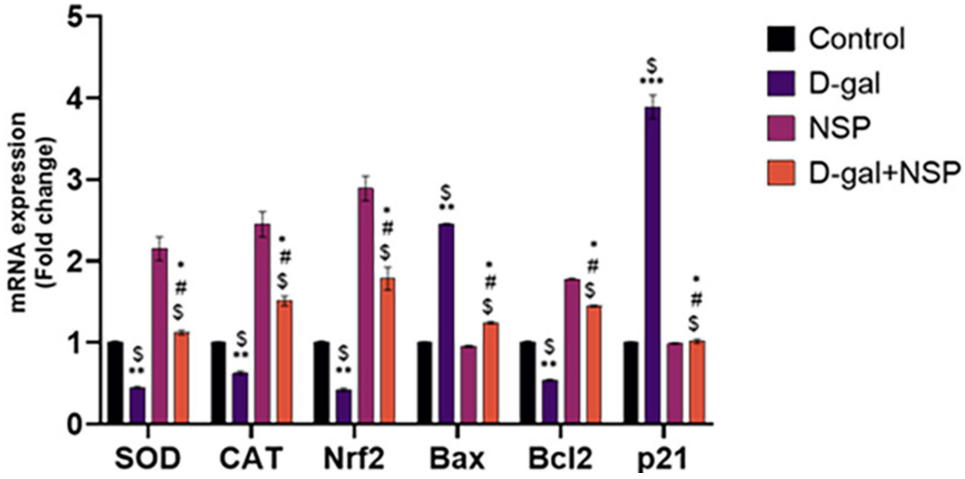

Figure 6 Brain SOD, CAT, Nrf2, Bax, BCl2, and p21 mRNA Expression after to the NSP Treatment. Data represented as Mean ± SE. *P < 0.05, **P < 0.01 vs the control. $P < 0.01 vs the NSP, #P <0.05 vs the D-gal. (n= 9).

those which increased in parallel to each other's such as MDA, ROS, AchE, CPK, γ-H2AX, P-P38MP, P-JNK, Bax, P21 levels. The negative correlation could be seen in the data set of increased parameters against those that show decreased levels in comeback to D-gal and/or NSP supplementation. In addition, Figure 7B summarizes the variable averages according to how they were treated in this study. These data suggest the occurrence of physiopathological alterations in D-gal-injured rats and the degree of improvements when co-administrated with NSP.

Then, to elucidate the most affecting variables in the present study, VIP scores were estimated. As shown in Figure 5C, Nrf2, CAT, SOD, Bcl2, Bax, P21, AchE, and JNK were the top contributing variables in the present study.

Histopathological and Immunohistochemical Assessment

The hippocampus of the control and NSP-treated group showed normal pyramidal cells, molecular cell layer, granular cell layer, and blood capillaries. In contrast, the aged rats showed aggregation of granular cells and pyramidal cells, area of demyelination and gliosis, nuclear pyknosis of some neurons, in addition to congested blood vessels and edema in

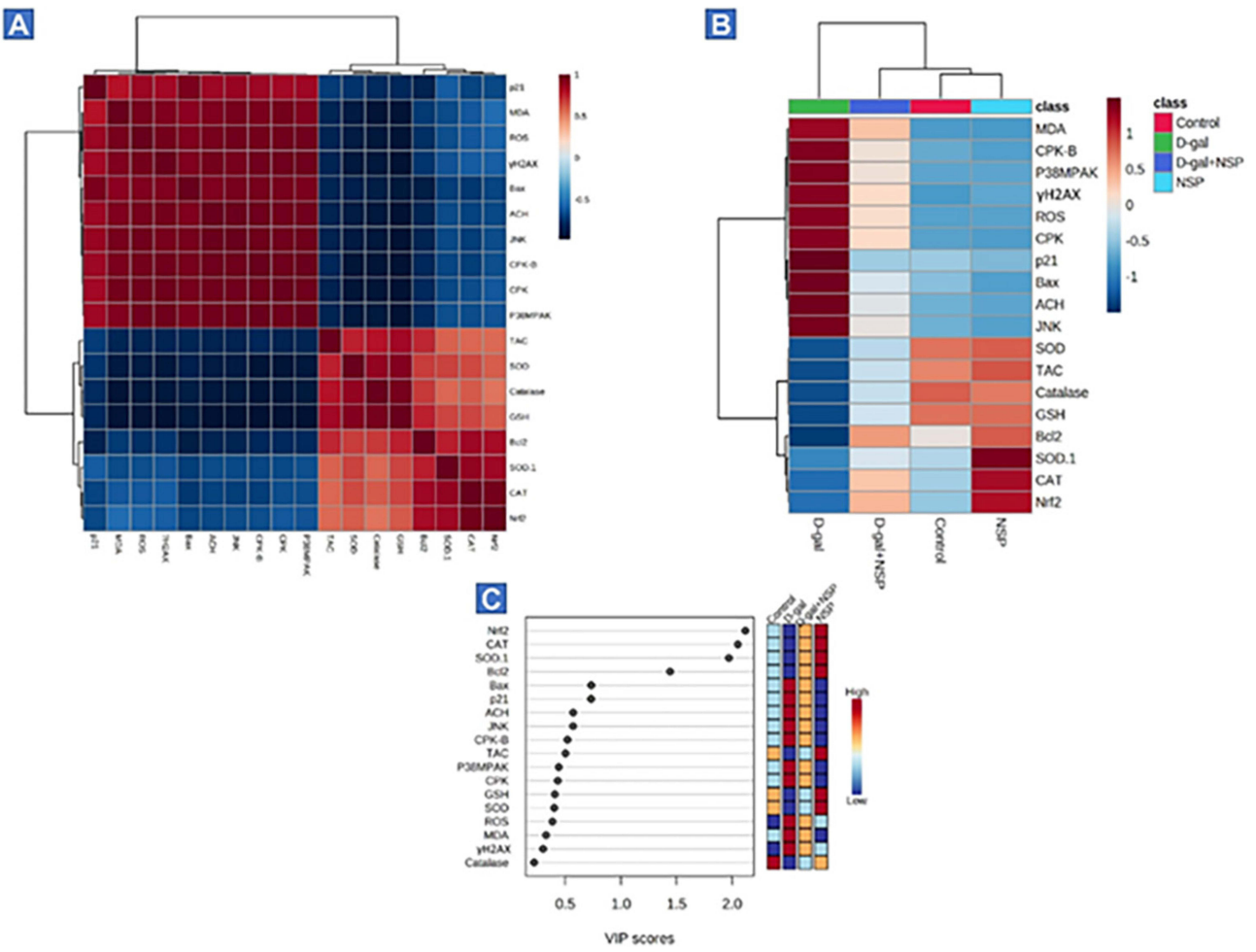

Figure 7 Analysis of the VIP ratings for all variables and their correlation heatmap (**A**) The correlation heatmap is a user-friendly data display that compiles the associations between biochemical variables and mRNA expression following D-gal and/or NSP administration. (**B**) The concentration values are shown as a heatmap generated by hierarchical clustering, with averages of each variable in the rows and the sets of treatments in the columns. Red denotes a positive association, and the scale runs from highest to lowest to illustrate the range of the contribution (blue indicates a negative correlation). The degree of correlation is shown by the color's intensity. The various squares are colored in accordance with Pearson's correlation coefficient between all measured variables. (**C**) Using variable importance in projection (VIP) scores, the boxes on the right show how each research group's measured parameters stack up in terms of concentration, with red being the highest concentration and blue the lowest (blue).

between pyramidal cells and neuronal degeneration with acidophilic cytoplasm. The NSP-treated aged rats showed granular cell layers with intact pyramidal cells and slightly dilated blood capillaries, as shown in Figure 8.

TEM panel of the hippocampus of the control and NSP treated groups showed a euchromatic nucleus of neuron, mitochondria in cytoplasm, myelinated axons, and rER, showing cell nuclei, abundant lysosome. In contrast, the TEM panel of the hippocampus of the aged rats showed astrocytes nucleus with peripheral heterochromatin, lysosomes surrounded by electron-lucent cytoplasm, asymmetric myelinated axons, and neurofilaments in addition to degenerated axons with slight demyelination and swelled mitochondria. The TEM of the NSP-treated aged rats showed swelled mitochondria with dilated rER and congested blood capillaries containing red blood cells and abundant lysosomes, as shown in Figure 9. The GFAP expression was significantly increased in the aged rats concerning the other examined groups, as shown in Figure 10.

Discussion

Losing organ and tissue function is a hallmark of aging.[29] The accumulation of oxidative damage to macromolecules (proteins, DNA, and lipids) by ROS and RNS is responsible for decreased age-related functions.[30] Senescent cells accumulate with age and have been linked to promoting several diseases associated with getting older.[31] As a result of senescence induction, p53 was activated, leading to an increase in p21(WAF1/CIP1), a cyclin-dependent kinase inhibitor that primarily mediates G1 growth

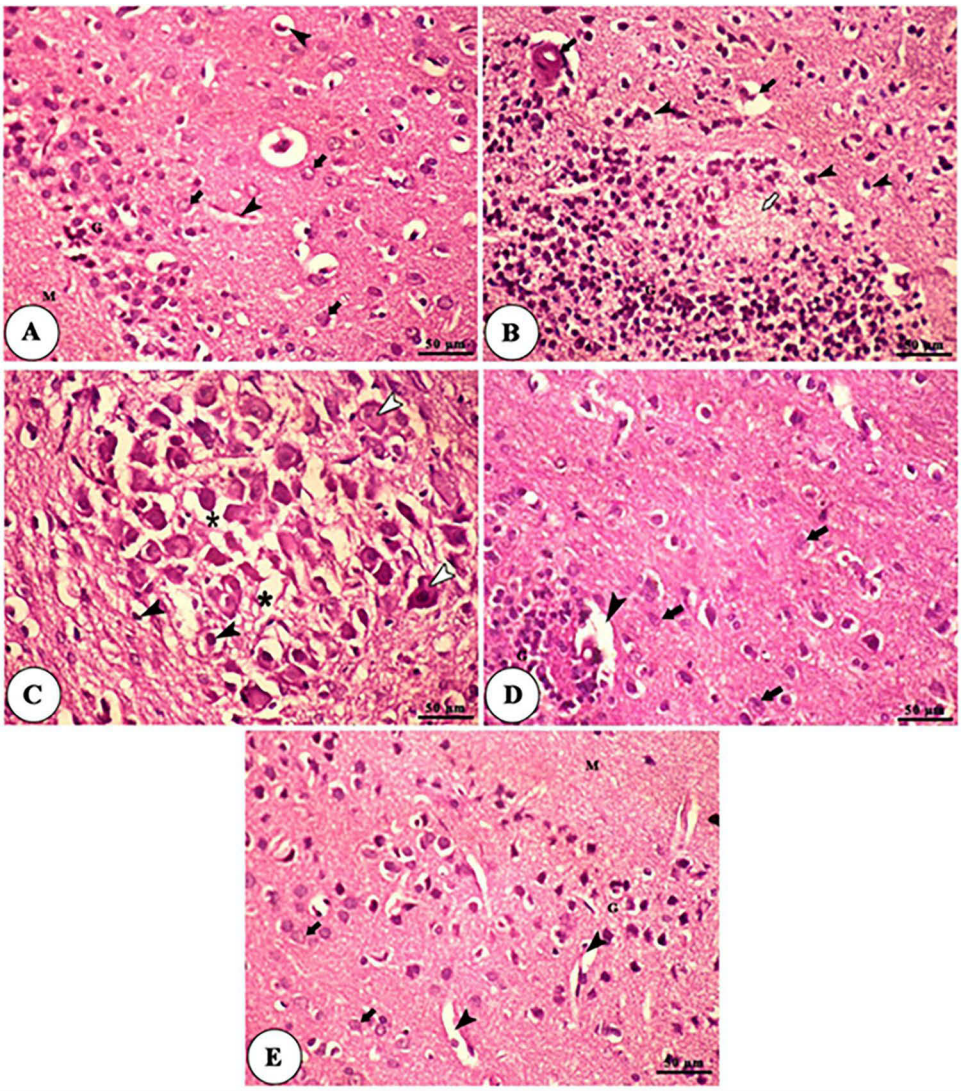

Figure 8 Histomicrograph of H&E-stained sections of the hippocampus of control (**A**), aged (**B** and **C**), NSP-treated aged rats (**D**), and NSP-treated groups (**E**). Plate A and E show the molecular cell layer (M), granular cell layer (G), pyramidal cells (black arrows), and blood capillaries (black arrowheads). Plate B shows an aggregation of granular cells (G), an area of demyelination and gliosis (white arrow), nuclear pyknosis of some neurons (black arrowheads) in addition to congested blood vessels (black arrows). Plate (C) shows an aggregation of pyramidal cells with pyknotic nuclei (black arrowheads), edema in between pyramidal cells (asterisk), and neuronal degeneration with acidophilic cytoplasm and pyknotic nuclei (white arrowheads). Plate (D) shows a granular cell layer (G), intact pyramidal cells (black arrows), and slightly dilated blood capillaries (black arrowheads).

arrest.[32] The ROS production, which drives inflammation and death of many bodily cells, is a well-established mechanism by which D-gal induces aging.[3,4] Therefore, it is essential to pinpoint the physiological mechanisms that contribute to healthy ageing and delay the onset of age-related disorders.[33] In vivo, investigations have shown that oxidative damage and the pro-inflammatory response are two major damaging processes that contribute to these defects.[34] In the current analysis, our result revealed that the d-gal-treated group significantly declined in body and brain weight. These results were in the same line as they reported the same finding in the rats and mice.[35,36]

The current study showed that supplementing D-gal-treated rats with NSP markedly restored body weight to near-normal quantities. These data jived with those of Ozdemir et al,[37] who showed that people with diabetes who had lost weight owing to protein breakdown in their tissues could put on the weight again after taking NSP. Benefits to weight increase may be attributable, due in part, to the rich nutritional profile provided by Arthrospira platensis, which includes protein, vitamin, mineral, and amino acid content.[38] The incredible efficiency with which Arthrospira platensis nano-particles are transported from circulation to their intended tissues and organs.[39]

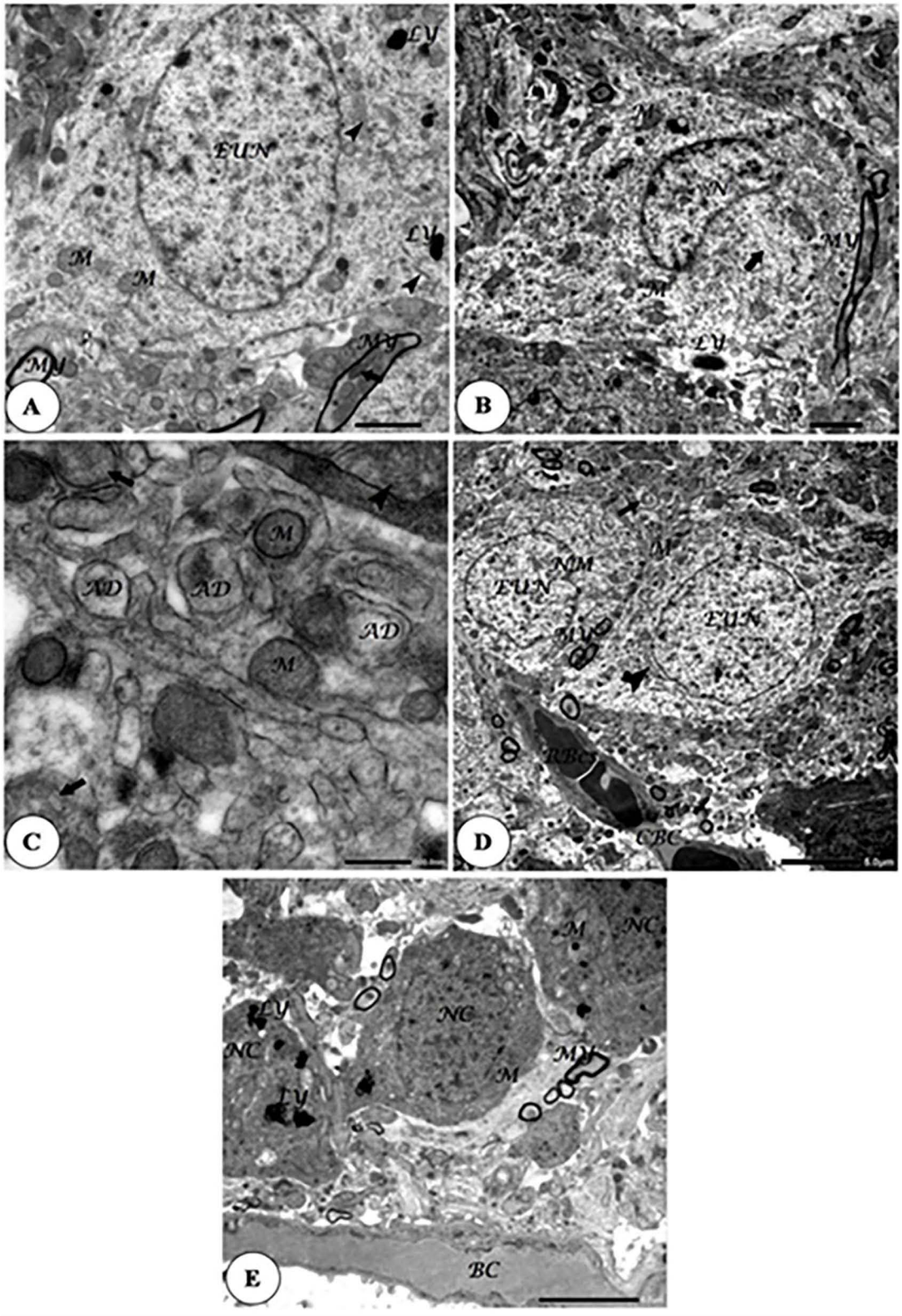

Figure 9 TEM panel of the hippocampus of control (**A**), aged (**B** and **C**), NSP-treated aged rats (**D**), and NSP-treated groups (**E**). Plate A showing the euchromatic nucleus of neuron (EUN), lysosomes (Ly), mitochondria in the cytoplasm (M) myelinated axons (My) contained mitochondria (black arrow), and rER (arrowhead). Plate B shows astrocytes nucleus with peripheral heterochromatin (N), lysosomes (Ly) surrounded by electron-lucent cytoplasm, asymmetric myelinated axons (My), and neurofilaments (black arrow). Plate (C) shows degenerated axons with slight demyelination (AD), swelled mitochondria (black arrows), and rER of adjacent neurons (arrowhead). Plate (D) shows swelled mitochondria (black arrows), dilated rER (black arrowhead), and congested blood capillaries (CBC) containing red blood cells (RBCs). Plate (E) showing cell nuclei (NC), abundant lysosomes (Ly), blood capillaries (BC), mitochondria (M), and myelinated axons (My).

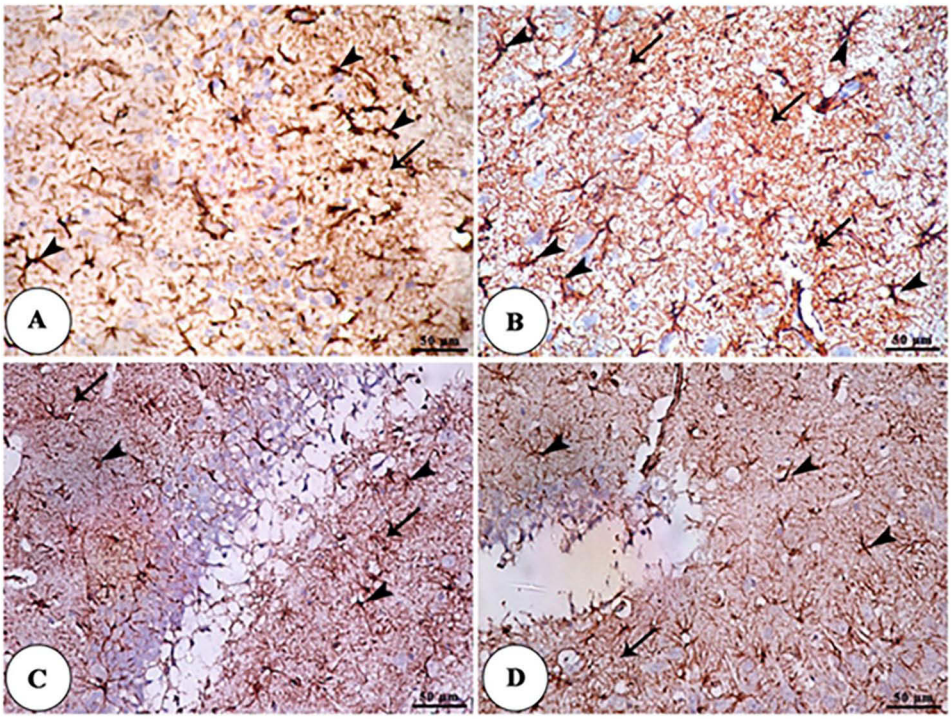

Figure 10 GFAP IHC panel of the hippocampus of control (**A**), aged (**B**), NSP-treated aged rats (**C**), and NSP-treated groups (**D**) showing increased expression of GFAP in astrocytes (arrowheads) and its processes (arrows) in the hippocampus of aged rats than the treated NSP and control groups.

In the current investigation, NSP dramatically reduced d-gal-induced oxidative stress in brain homogenates. By bringing MDA and ROS levels back to normal, as shown in Figure 1, NSP significantly boosted the activities of SOD, Catalases, and the total antioxidant capacity. Additionally, our result concerning the oxidative stress of the d-gal was supported by Elabd et al,[40] in which the D-gal administration induces aging by increasing oxidative injury with subsequent apoptosis and inflammation. Multiple organs are vulnerable to the aging effects of exogenous d-gal because it promotes oxidative stress, apoptosis, and inflammation.[41] The brain is particularly susceptible to oxidant stress due to its high-fat content, rapid metabolism, and inadequate antioxidant defenses.[42]

In the same way, our findings showed a significant increase in brain acetylcholinesterase activity, which may have been caused by a rise in lipid peroxidation brought on by the breakdown of cell membranes.[43] Our finding was in harmony with Kumar et al and Xian et al[44,45] In addition, Abdel-Daim et al,[46] revealed that Arthrospira platensis restored the increased level of ACHE induced by the sub-acute toxicity of deltamethrin in mice. In the D-gal-treated group, we observed statistically significant serum CPK and CPK-BB elevations. That correlated with brain damage associated with free radical-cell interaction, ultimately resulting in cell damage. This finding was in line with El-Far et al,[40] who reported that the CPK and CPK-BB were markers of aging.

Age-related neurodegeneration is mainly due to DNA damage.[47] As well as, D-gal-induced boosts the γ-H2AX molecules that reconcile DNA damage. In addition,[48] showed that The anti-aging effect might be mediated by the prevention of DNA damage, which supports our finding concerning the brain γ-H2AX level that markedly increased by D-gal administration and restored by the NSP treatment near to the normal level, which was confirmed by Amadeu etal.,[49] that proved the decreased level of the γ-H2AX after Arthrospira platensis administration.

Increased phosphorylation levels of p38MAPK and JNK were observed after the NSP treatment restored d-gal administration. Considering these findings, the MAPK pathway appears to be a promising therapeutic target for treating brain injury. This result was supported by Trotta and Porro [50] They showed that the Arthrospira platensis squelched the phosphorylation of p38 MAPK, SAPK/JNK, and JNK.

We compared the effects of NSP and D-gal on cellular senescence and apoptosis in the current investigation. Our result has proven that the D-gal administration substantially downregulated the mRNA expression of the SOD, Catalase, GSH, and Nrf2, which was in line with, Atef et al,[51] who reported the oxidative injury of the D-gal. Our data revealed that NSP treatment restored

this effect, which was in harmony with Shaman et al,[17] which said the antioxidant impact of the *A. platensis* Nanoparticles. In the current investigation, the mRNA expression of the Bax was extensively upregulated with marked down-regulation of the Bcl2 by the D-gal treatment. Many prior research studies have shown similar results.[52,53] This effect was restored by the NSP treatment, consistent with, Shaman et al,[17] who proved the anti-apoptotic effect of the *A. platensis*. D-gal injection triggered a dramatic increase in p21 mRNA expression in the brain. This was in harmony with El-Far et al[40] D-gal causes oxidative stress due to the production of reactive oxygen species (ROS) and the inhibition of antioxidant enzyme activity.[54] The NSP treatment restored the upregulation effect of d-gal to p21 mRNA expression.

Our previous data was supported by the histopathological analysis and TEM panel of the hippocampus in addition to the significant expression of the GFAP in the aged rat, which significantly normalized with NSP treatment. Our result was in harmony with, Venkateshappa et al,[55] which showed that GFAP expression rises with age, potentially making the brain more susceptible to neurotoxic assaults. In addition, Zhou et al,[56] revealed that *Aspergillus platensis* reduced GFAP levels via the gut-brain axis in high-fat-diet-induced memory loss in mice.

The multivariate analyses represented by heatmaps and VIP scores affirm the abovementioned data. The clustering heatmap revealed apparent differences in concentration values between NSP- and D-gal-treated mice. These results provide substantial evidence that NSP has anti-aging benefits for brain tissue. The VIP scores revealed that the Nrf2, CAT, SOD, Bcl2, Bax, P21, AchE, and JNK were the top contributing variables in such protective mechanisms. Moreover, these markers could be potentially used as diagnostic markers for monitoring the defensive efficiency of NSP in aged brain tissue.

Conclusions and Prospects

Despite the new evidence, the oxidative stress theory of age-related cellular changes is still a strong contender. NSP may have mitigated the oxidative injury generated by d-gal in rat brains by lowering aging and apoptotic markers and increasing antioxidant status a possible mechanism of NSP action via mitogen-activated protein kinase. Our findings suggest NSP may be an effective natural anti-aging supplement for reducing age-related indicators in rat brain tissues.

Data Sharing Statement

Available upon request from the corresponding author.

Ethics Statement

The Faculty of Veterinary Medicine, Kafrelsheikh University, Egypt approved the experimental methods procedure.

Acknowledgments

The authors thank the Deanship of Scientific Research at King Khalid University for funding this work through a large group Research Project under grant number RGP2/435/44. The authors also extend their considerations for the outstanding support offered by the Princess Nourah bint Abdulrahman University Researchers Supporting Project number (PNURSP2023R127), Princess Nourah bint Abdulrahman University, Riyadh, Saudi Arabia. The authors thank the resources provided by the project 6PFE of the University of Life Sciences "King Mihai I" from Timisoara and the Research Institute for Biosecurity and Bioengineering from Timisoara.

Author Contributions

All authors made a significant contribution to the work reported, whether that is in the conception, study design, execution, acquisition of data, analysis and interpretation, or in all these areas; took part in drafting, revising or critically reviewing the article; gave final approval of the version to be published; have agreed on the journal to which the article has been submitted; and agree to be accountable for all aspects of the work.

Funding

The authors thank the Deanship of Scientific Research at King Khalid University for funding this work through a large group Research Project under grant number RGP2/435/44. The authors also extend their appreciations to all support provided by the Princess Nourah bint Abdulrahman University Researchers Supporting Project number (PNURSP2023R127), Princess Nourah

bint Abdulrahman University, Riyadh, Saudi Arabia. The authors thank the resources provided by the project 6PFE of the University of Life Sciences "King Mihai I" from Timisoara and the Research Institute for Biosecurity and Bioengineering from Timisoara.

Disclosure

The authors report no conflicts of interest in this work.

References

1. Chen Y, Peng Y, Xu H, O'Brien WH. Age differences in stress and coping: problem-focused strategies mediate the relationship between age and positive affect. *Int J Aging Human Dev*. 2018;86(4):347–363. doi:10.1177/0091415017720890
2. Liu P, Zhao H, Luo Y. Anti-aging implications of Astragalus membranaceus (Huangqi): a well-known Chinese tonic. *Aging Dis*. 2017;8(6):868. doi:10.14336/AD.2017.0816
3. Hegab Z, Gibbons S, Neyses L, Mamas MA. Role of advanced glycation end products in cardiovascular disease. *World J Cardiol*. 2012;4(4):90. doi:10.4330/wjc.v4.i4.90
4. Frimat M, Daroux M, Litke R, Nevière R, Tessier FJ, Boulanger E. Kidney, heart and brain: three organs targeted by ageing and glycation. *Clin Sci*. 2017;131(11):1069–1092.
5. Vivarelli S, Falzone L, Basile MS, Candido S, Libra M. Nitric oxide in hematological cancers: partner or rival? *Antioxid Redox Signal*. 2021;34 (5):383–401. doi:10.1089/ars.2019.7958
6. Singh A, Kukreti R, Saso L, Kukreti S. Oxidative stress: a key modulator in neurodegenerative diseases. *Molecules*. 2019;24(8):1583. doi:10.3390/ molecules24081583
7. Singh D, Singh M, Yadav E, et al. Attenuation of diethylnitrosamine (DEN)–Induced hepatic cancer in experimental model of Wistar rats by Carissa carandas embedded silver nanoparticles. *Biomed Pharmacother*. 2018;108:757–765. doi:10.1016/j.biopha.2018.09.066
8. Mabrouk MM, Ashour M, Labena A, et al. Nanoparticles of Arthrospira platensis improves growth, antioxidative and immunological responses of Nile tilapia (Oreochromis niloticus) and its resistance to Aeromonas hydrophila. *Aquaculture Res*. 2021.
9. Parvatkar RR, D'Souza C, Tripathi A, Naik CG. Aspernolides A and B, butenolides from a marine-derived fungus Aspergillus terreus. *Phytochemistry*. 2009;70(1):128–132. doi:10.1016/j.phytochem.2008.10.017
10. Saleh AA, Eid YZ, Ebeid TA, et al. The modification of the muscle fatty acid profile by dietary supplementation with Aspergillus awamori in broiler chickens. *Br J Nutr*. 2012;108(9):1596–1602. doi:10.1017/s0007114511007069
11. Fox EM, Howlett BJ. Secondary metabolism: regulation and role in fungal biology. *Curr Opin Microbiol*. 2008;11(6):481–487. doi:10.1016/j. mib.2008.10.007
12. Salar RK, Purewal SS, Sandhu KS. Bioactive profile, free-radical scavenging potential, DNA damage protection activity, and mycochemicals in Aspergillus awamori (MTCC 548) extracts: a novel report on filamentous fungi. *3 Biotech*. 2017;7(3):1–9. doi:10.1007/s13205-017-0834-2
13. Niemiec T, Łozicki A, Pietrasik R, et al. Impact of Ag nanoparticles (AgNPs) and multimicrobial preparation (EM) on the carcass, mineral, and fatty acid composition of *Cornu aspersum aspersum* snails. *Animals*. 2021;11(7):1926. doi:10.3390/ani11071926
14. Atta MS, Almadaly EA, El-Far AH, et al. Thymoquinone defeats diabetes-induced testicular damage in rats targeting antioxidant, inflammatory and aromatase expression. *Int J Mol Sci*. 2017;18(5):919. doi:10.3390/ijms18050919
15. Fan J, Yang X, Li J, et al. Spermidine coupled with exercise rescues skeletal muscle atrophy from D-gal-induced aging rats through enhanced autophagy and reduced apoptosis via AMPK-FOXO3a signal pathway. *Oncotarget*. 2017;8(11):17475. doi:10.18632/oncotarget.15728
16. Feng W, Liu J, Wang S, et al. Alginate oligosaccharide alleviates D-galactose-induced cardiac ageing via regulating myocardial mitochondria function and integrity in mice. *J Cell Mol Med*. 2021;25(15):7157–7168. doi:10.1111/jcmm.16746
17. Shaman AA, Zidan NS, Atteia HH, et al. Arthrospira platensis nanoparticles defeat against diabetes-induced testicular injury in rat targeting, oxidative, apoptotic, and steroidogenesis pathways. *Andrologia*. 2022;54(8):e14456. doi:10.1111/and.14456
18. Beutler E, Duron O, Kelly BM. Improved method for the determination of blood glutathione. *J Lab Clin Med*. 1963;61:882–888.
19. Flohe L. Superoxide dismutase assays. *Methods Enzymology Elsevier*. 1984;93–104.
20. Aebi H. [13] Catalase in vitro. In: *Methods in Enzymology*. Elsevier; 1984. 121–126.
21. Koracevic D, Koracevic G, Djordjevic V, Andrejevic S, Cosic V. Method for the measurement of antioxidant activity in human fluids. *J Clin Pathol*. 2001;54(5):356–361. doi:10.1136/jcp.54.5.356
22. Ohkawa H, Ohishi N, Yagi K. Assay for lipid peroxides in animal tissues by thiobarbituric acid reaction. *Anal Biochem*. 1979;95(2):351–358. doi:10.1016/0003-2697(79)90738-3
23. Den Blaauwen D, Poppe W, Tritschler W. Cholinesterase (EC 3.1. 1.8) with butyrylthiocholine-iodide as substrate: references depending on age and sex with special reference to hormonal effects and pregnancy. *J Clin Chem Clin Biochem*. 1983;21(6):381–386.
24. Socci D, Bjugstad K, Jones H, Pattisapu J, Arendash G. Evidence that oxidative stress is associated with the pathophysiology of inherited hydrocephalus in the H-Tx rat model. *Exp Neurol*. 1999;155(1):109–117. doi:10.1006/exnr.1998.6969
25. Bradford MM. A rapid and sensitive method for the quantitation of microgram quantities of protein utilizing the principle of protein-dye binding. *Anal Biochem*. 1976;72(1–2):248–254. doi:10.1016/0003-2697(76)90527-3
26. Livak KJ, Schmittgen TD. Analysis of relative gene expression data using real-time quantitative PCR and the 2− ΔΔCT method. *Methods*. 2001;25 (4):402–408. doi:10.1006/meth.2001.1262
27. Bancroft JD, Layton C. The hematoxylins and eosin. *Bancroft's Theory Practice Histological Techniques*. 2012;173–186.
28. Malkiewicz K, Koteras M, Folkesson R, et al. Cypermethrin alters glial fibrillary acidic protein levels in the rat brain. *Environ Toxicol Pharmacol*. 2006;21(1):51–55. doi:10.1016/j.etap.2005.06.005
29. Flatt T. A new definition of aging? *Front Genet*. 2012;3:148. doi:10.3389/fgene.2012.00148
30. Beckman KB, Ames BN. The free radical theory of aging matures. *Physiol Rev*. 1998;78(2):547–581. doi:10.1152/physrev.1998.78.2.547
31. Regulski MJ. Cellular senescence: what, why, and how. *Wounds*. 2017;29(6):168–174.

32. Galanos P, Vougas K, Walter D, et al. Chronic p53-independent p21 expression causes genomic instability by deregulating replication licensing. *Nat Cell Biol*. 2016;18(7):777–789. doi:10.1038/ncb3378
33. Le Couteur DG, McLachlan AJ, Quinn RJ, Simpson SJ, de Cabo R. Aging biology and novel targets for drug discovery. *J Gerontol Series A*. 2012;67(2):168–174.
34. Lotze MT, Zeh HJ, Rubartelli A, et al. The grateful dead: damage-associated molecular pattern molecules and reduction/oxidation regulate immunity. *Immunol Rev*. 2007;220(1):60–81.
35. Chen P, Chen F, Zhou B. Antioxidative, anti-inflammatory and anti-apoptotic effects of ellagic acid in liver and brain of rats treated by D-galactose. *Sci Rep*. 2018;8(1):1–10.
36. Suo H, Liu S, Li J, et al. Lactobacillus paracasei ssp. paracasei YBJ01 reduced d-galactose–induced oxidation in male Kuming mice. *J Dairy Sci*. 2018;101(12):10664–10674. doi:10.3168/jds.2018-14758
37. Ozdemir O, Akalin PP, Baspinar N, Hatipoglu F. Pathological changes in the acute phase of streptozotocin-induced diabetic rats. *Bull Vet Inst Pulawy*. 2009;53(4):783–790.
38. Barkallah M, Ben Slima A, Elleuch F, et al. Protective role of Spirulina platensis against bifenthrin-induced reprotoxicity in adult male mice by reversing expression of altered histological, biochemical, and molecular markers including microRNAs. *Biomolecules*. 2020;10(5):753. doi:10.3390/biom10050753
39. Elabd H, Wang H-P, Shaheen A, Matter A. Nano spirulina dietary supplementation augments growth, antioxidative and immunological reactions, digestion, and protection of Nile tilapia, Oreochromis niloticus, against Aeromonas veronii and some physical stressors. *Fish Physiol Biochem*. 2020;46(6):2143–2155.
40. El-Far AH, Mohamed HH, Elsabagh DA, et al. Eugenol and carvacrol attenuate brain d-galactose-induced aging-related oxidative alterations in rats. *Environ Sci Pollution Res*. 2022;1–12.
41. Rehman SU, Shah SA, Ali T, Chung JI, Kim MO. Anthocyanins reversed D-galactose-induced oxidative stress and neuroinflammation mediated cognitive impairment in adult rats. *Mol Neurobiol*. 2017;54(1):255–271.
42. Çakatay U. *Protein Redox-Regulation Mechanisms in Aging. Aging and Age-Related Disorders*. Springer; 2010:3–25.
43. Kaizer RR, Corrêa MC, Spanevello RM, et al. Acetylcholinesterase activation and enhanced lipid peroxidation after long-term exposure to low levels of aluminum on different mouse brain regions. *J Inorg Biochem*. 2005;99(9):1865–1870. doi:10.1016/j.jinorgbio.2005.06.015
44. Kumar A, Dogra S, Prakash A. Protective effect of curcumin (Curcuma longa), against aluminium toxicity: possible behavioral and biochemical alterations in rats. *Behav Brain Res*. 2009;205(2):384–390.
45. Xian Y-F, Lin Z-X, Zhao M, Mao -Q-Q, S-P I, Che C-T. Uncaria rhynchophylla ameliorates cognitive deficits induced by D-galactose in mice. *Planta Med*. 2011;77(18):1977–1983. doi:10.1055/s-0031-1280125
46. Abdel-Daim M, El-Bialy BE, Rahman HGA, Radi AM, Hefny HA, Hassan AM. Antagonistic effects of Spirulina platensis against sub-acute deltamethrin toxicity in mice: biochemical and histopathological studies. *Biomed Pharmacother*. 2016;77:79–85.
47. Lam J, McKeague M. Dietary modulation of mitochondrial DNA damage: implications in aging and associated diseases. *J Nutr Biochem*. 2019;63:1–10.
48. Xu D, Yang J, Yu W, Wei J. Anthocyanins from black chokeberry delayed ageing-related degenerative changes in the heart. *Indian J Pharm Educ*. 2019;53:112–116. doi:10.5530/ijper.53.1.15
49. Amadeu SO, Sarmiento-Machado LM, Bartolomeu AR, et al. Arthrospira (Spirulina) platensis feeding reduces the early stage of chemically induced rat colon carcinogenesis. *Br J Nutrition*. 2022;1–11.
50. Trotta T, Porro C, Cianciulli A, Panaro MA. Beneficial effects of spirulina consumption on brain health. *Nutrients*. 2022;14(3):676. doi:10.3390/nu14030676
51. Atef MM, Emam MN, Abo El Gheit RE, et al. Mechanistic Insights into Ameliorating Effect of Geraniol on D-Galactose Induced Memory Impairment in Rats. *Neurochem Res*. 2022;47(6):1664–1678. doi:10.1007/s11064-022-03559-3
52. Shahroudi MJ, Mehri S, Hosseinzadeh H. Anti-aging effect of Nigella sativa fixed oil on D-galactose-induced aging in mice. *J Pharmacopuncture*. 2017;20(1):29. doi:10.3831/KPI.2017.20.006
53. L-Q X, Xie Y-L, Gui S-H, et al. Polydatin attenuates d-galactose-induced liver and brain damage through its anti-oxidative, anti-inflammatory and anti-apoptotic effects in mice. *Food Funct*. 2016;7(11):4545–4555. doi:10.1039/C6FO01057A
54. Xu Y, Wu T, Jin Y, Fu Z. Effects of age and jet lag on D-galactose induced aging process. *Biogerontology*. 2009;10(2):153–161. doi:10.1007/s10522-008-9158-2
55. Venkateshappa C, Harish G, Mythri RB, Mahadevan A, Srinivas Bharath M, Shankar S. Increased oxidative damage and decreased antioxidant function in aging human substantia nigra compared to striatum: implications for Parkinson's disease. *Neurochem Res*. 2012;37(2):358–369. doi:10.1007/s11064-011-0619-7
56. Zhou T, Liu Y, Wang Q, et al. Spirulina platensis alleviates high fat diet-induced cognitive impairment in mice via the gut-brain axis. *J Funct Foods*. 2021;86:104706. doi:10.1016/j.jff.2021.104706